

MECHANICAL VIBRATIONS IN THERMORHEOLOGICALLY SIMPLE VISCOELASTIC BEAMS AND PLATES

R. D. MARANGONI

Department of Mechanical Engineering, University of Pittsburgh, Pittsburgh, PA 15261, U.S.A.

and

NAGESH BASAVANHALLY

Schneider Consulting Engineers, Bridgeville, PA 15017, U.S.A.

(Received 16 July 1981; in revised form 10 February 1982)

Abstract—The problem of vibration of viscoelastic beams and plates subjected to a known transient temperature distribution and simply supported boundary conditions has been solved using a Williams-type modal expansion technique. The viscoelastic property ascribed is linear but otherwise general and its temperature dependence follows a thermorheologically simple viscoelastic law. The internal damping considered is proportional to the velocity of motion. The measured material relaxation has been characterized using a Dirichlet Series which represents a Maxwell chain. The analytical solution is based upon superposing a time dependent "static" problem that contains the time-varying boundary conditions and a "reduced dynamic" problem that contains the inertia terms and the homogeneous boundary conditions. The integro-differential equation that results from the dynamic problem has been solved numerically using a fourth order Runge-Kutta method. Typical results are presented for epoxy resin and float glass. The numerical data required are measured for epoxy resin and taken from published viscoelastic properties for float glass. The experimentally measured free vibration response of epoxy resin beams at different but constant temperature has been compared with the theoretically developed model.

1. INTRODUCTION

The mechanical vibration of a viscoelastic material introduces the effect of change in the material properties with time and temperature, and the dissipation of energy due to periodic variation of the applied stress level. Because of the change in properties with temperature, any temperature distribution through the material will result in material properties being functions of the space co-ordinates. The viscoelastic material property can be represented by Voigt, Maxwell or Standard Linear Solid Models[1]. The limitation of these models is that they have only one relaxation and retardation time. Since the real materials have a continuous relaxation and retardation spectra, the material characterization can be improved by taking combinations of the above said models. In the present analysis a Dirichlet series which represents a Maxwell chain[2, 3] has been used. This representation avoids the storage of history effects and replaces it by a simple recursion formula[4]. Daniel[5] has experimentally concluded that Poisson's ratio remains essentially a constant during wave propagation through viscoelastic materials. Also, Winter[6] has experimentally shown that the Poisson's ratio is relatively a constant for high performance epoxy resins that are viscoelastic in nature. This hypothesis of constant Poisson's ratio has been used in this analysis.

Valanis[7] has shown that the solution to a viscoelastic vibration problem can be obtained by superimposing a "static problem" and a "reduced dynamic problem". This method is restricted to a constant Poisson's ratio and a separable form of boundary conditions. Robertson[8] has used this technique to solve the forced motion of a viscoelastic circular plate. Another technique based on William's method, first used for solving the forced motion of elastic beams[9, 10] was generalized by Reismann[11] to elastic continua. Robertson[12] used this technique to solve the forced motion of viscoelastic circular plates. This method which allows time varying tractions and displacement on the boundary as well as time varying body forces was extended to viscoelastic media by Robertson and Thomas[13]. All the work mentioned here are restricted to a uniform temperature through the body. In the present work the Williams method has been used to accommodate the time varying boundary conditions resulting from the transient temperature distribution.

Almost all materials dissipate energy during cyclic loading. For materials which dissipate

energy, the cyclic load deformation curve forms a hysteretic loop. The area enclosed by such a loop is a measure of damping or energy dissipation of the material. For viscoelastic materials the damping has a direct relation to frequency and temperature. Lazan[14] has discussed the effect of temperature on damping. The material properties available in the literature are the relaxation and creep data at different temperatures that are obtained by static experiments. In the present analysis statically measured relaxation data has been used. Also to include the damping effect due to cyclic loading, an equivalent viscous damping model has been developed for both beams and plates (see Appendix A). The viscous damping model which assumes the damping force, a function of frequency, to be proportional to the velocity has been shown by Bandstra[15] to be fairly accurate up to 10% of critical damping. This covers a large percentage of damping found in real life problems.

2. THEORY

2.1 Equation of motion for thermoviscoelastic beams and plates

Morland and Lee[16] included the general case of a temperature field $T(x_k)$ in the constitutive equation for a thermoheologically simple material as

$$S_{ij}(x_k, t) = \int_{-\infty}^t 2G[\xi(x_k, t) - \xi(x_k, t')] \frac{\partial}{\partial t'} e_{ij}(x_k, t') dt' \quad (2.1)$$

defining the deviatoric stress component and

$$\sigma(x_k, t) = \int_{-\infty}^t 3K[\xi(x_k, t) - \xi(x_k, t')] \frac{\partial}{\partial t'} \{\epsilon(x_k, t') - 3\alpha_0\theta(x_k, t')\} dt' \quad (2.2)$$

the volumetric stress component with the "reduced time" as

$$\xi(x_k, t) = \int_0^t \phi[T(x_k, t')] dt' \quad (2.3)$$

and "pseudo temperature"

$$\theta(x_k, t) = \frac{1}{\alpha_0} \int_{T_0}^{T(x_k, t)} \alpha(T') dt'; \quad \alpha_0 = \alpha(T_0) \quad (2.4)$$

where T_0 is the unstressed temperature state. The pseudo temperature is introduced to account for varying coefficients of thermal expansion. $G(\xi)$ and $K(\xi)$ are respectively the relaxation modulus in shear and dilatation. The shift factor $\phi(T)$ is an intrinsic material property which must be obtained experimentally.

For the beam element shown in Fig. 1 it can be easily shown using equilibrium, constitutive and compatibility equations that

$$\begin{aligned} -2b(1+\nu) \int_{-h/2}^{h/2} z^2 \frac{\partial^2}{\partial x^2} \left\{ G(\xi - \xi') * \frac{\partial^2 w}{\partial x^2} \right\} dz - b\alpha_0 \int_{-h/2}^{h/2} z \frac{2(1+\nu)}{(1-2\nu)} \frac{\partial^2}{\partial x^2} \\ \{ 3G(\xi - \xi') * \theta \} dz + q(x, t) = \rho A \frac{\partial^2 w}{\partial t^2} + C_b \frac{\partial w}{\partial t} \end{aligned} \quad (2.5)$$

is the equation of motion for the transverse vibration of a thermoviscoelastic beam where

$$f * g = \int_{-\infty}^t f(t - \tau) \frac{\partial g(\tau)}{\partial \tau} d\tau.$$

C_b = the equivalent viscous damping per unit length; and ν = Poisson's Ratio (taken to be a constant).

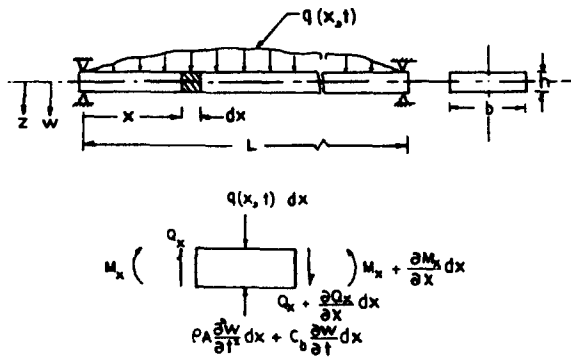


Fig. 1. Co-ordinate system used in the beam analysis.

The boundary conditions for a simply supported beam are

$$W = 0$$

and

$$\int_{-h/2}^{h/2} G * z^2 \frac{\partial^2 w}{\partial x^2} dz + \frac{1}{(1-2\nu)} \int_{-h/2}^{h/2} G * (3\alpha_0 \theta) z dz = 0 \tag{2.6}$$

at $x = 0$ and $x = L$. This is valid for arbitrary initial conditions.

Similarly for the set of co-ordinates considered in Fig. 2 the equation of motion for a viscoelastic simply supported plate can be shown to be

$$\begin{aligned} & -\frac{12}{h^3} \int_{-h/2}^{h/2} z^2 \frac{\partial^2}{\partial x^2} \left\{ D(\xi - \xi') * \left(\frac{\partial^2 w}{\partial x^2} + \nu \frac{\partial^2 w}{\partial y^2} \right) \right\} dz - \frac{12}{h^3} \int_{-h/2}^{h/2} z^2 \frac{\partial^2}{\partial y^2} \left\{ D(\xi - \xi') * \right. \\ & \left. \left(\frac{\partial^2 w}{\partial y^2} + \nu \frac{\partial^2 w}{\partial x^2} \right) \right\} dz - \nabla^2 \int_{-h/2}^{h/2} \frac{12}{h^3} (1 + \nu) D(\xi - \xi') * (z\alpha_0 \theta) dz - \frac{24}{h^3} \\ & \int_{-h/2}^{h/2} z^2 (1 - \nu) \frac{\partial^2}{\partial x \partial y} \left\{ D(\xi - \xi') * \frac{\partial^2 w}{\partial x \partial y} \right\} dz + q'(x, y, t) = \rho h \frac{\partial^2 w}{\partial t^2} + C_p \frac{\partial w}{\partial t} \end{aligned} \tag{2.7}$$

where

$$D(\xi - \xi') = \frac{2\mu(\xi - \xi')h^3}{12(1 - \nu)}$$

and C_p = the equivalent viscous damping per unit area. The boundary conditions for a simply supported plate are

$$W = 0,$$

$$\int_{-h/2}^{h/2} D * \frac{\partial^2 w}{\partial x^2} z^2 dz + \int_{-h/2}^{h/2} D * \frac{(1 + \nu)}{3} \cdot 3\alpha_0 \theta \cdot z dz = 0$$

on $x = 0$ and $x = a$, and

$$W = 0$$

$$\int_{-h/2}^{h/2} D * \frac{\partial^2 w}{\partial y^2} z^2 dz + \int_{-h/2}^{h/2} D * \frac{(1 + \nu)}{3} 3\alpha_0 \theta z dz = 0 \tag{2.8}$$

on $y = 0$ and $y = b$. This is valid for arbitrary initial conditions.

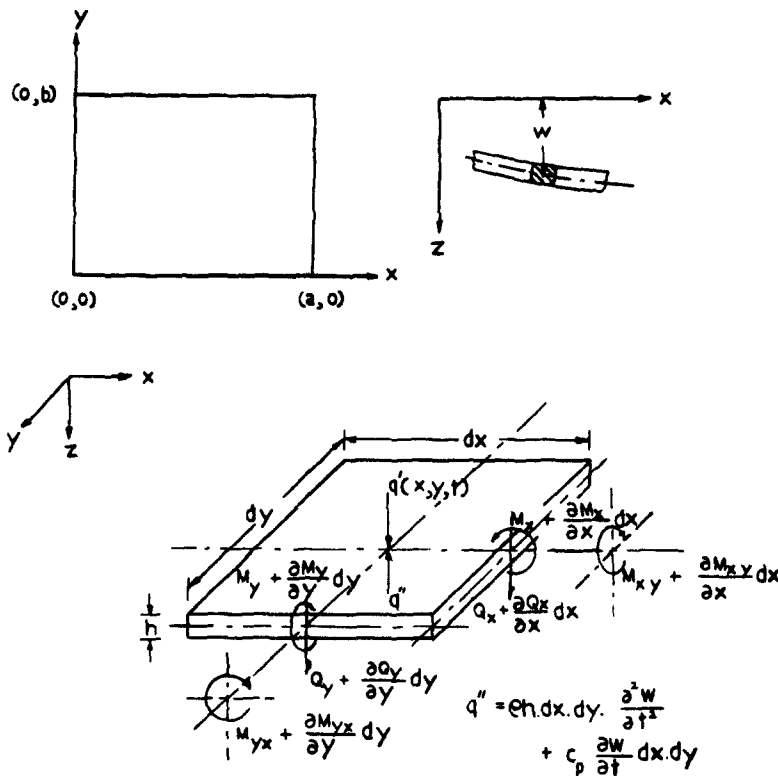


Fig. 2. Co-ordinate system used in the plate analysis.

3. HEAT CONDUCTION THROUGH A SLAB

The field equation for temperature distribution due to conduction of heat through a slab is given by [17]

$$\frac{\partial^2 T}{\partial z^2} = \frac{1}{\bar{\alpha}} \cdot \frac{\partial T}{\partial t} \tag{3.1}$$

where $\bar{\alpha}$ is the thermal diffusivity. The boundary and initial conditions considered respectively are

$$T(-h/2, t) = T_2$$

$$T(h/2, t) = T_1$$

and

$$T(z, 0) = T_1. \tag{3.2}$$

The solution to the above problem is

$$\theta = T - T_1 = (T_2 - T_1) \left[\frac{1}{2}(1 - \bar{z}) - \frac{2}{\pi} \sum_n \frac{1}{n} \exp\left(\frac{-n^2 \pi^2 \bar{\alpha} t}{h^2}\right) \sin \frac{n\pi}{2} (\bar{z} + 1) \right]$$

where

$$\bar{z} = 2 \frac{z}{h}. \tag{3.3}$$

4. SOLUTION TO THE EQUATION OF MOTION OF THERMOVISCOELASTIC BEAMS AND PLATES

4.1 Solution to the equation of motion of a beam

For the temperature distribution given in Section 3, the equation of motion (2.5) reduces to

$$\int_{-1}^{+1} \bar{z}^2 \cdot G * \frac{\partial^4 w}{\partial \eta^4} d\bar{z} = - \frac{4\rho AL^4}{bh^3(1+\nu)} \cdot \frac{\partial^2 w}{\partial t^2} - \frac{4L^4}{bh^3(1+\nu)} C_b \frac{\partial w}{\partial t} \quad (4.1)$$

where $\bar{z} = 2z/h$ and $\eta = x/L$. The boundary conditions are

$$w = 0$$

and

$$\int_{-1}^{+1} \bar{z} \cdot G * \left\{ \frac{(1-2\nu)h}{2L^2} \bar{z} \frac{\partial^2 w}{\partial \eta^2} \right\} d\bar{z} = -3\alpha_0 \int_{-1}^{+1} \bar{z} G * \theta dz \quad (4.2)$$

at $\eta = 0$ and $\eta = 1$.

The solution to the eqn (4.1) can be written as [13]

$$w(\eta, t) = U(\eta, t) + \sum_{m=1}^{\infty} v^{(m)}(\eta) \cdot q_m(t) \quad (4.3)$$

where U the "static solution" satisfies

$$\int_{-1}^{+1} \bar{z}^2 G * \frac{\partial^4 U}{\partial \eta^4} d\bar{z} = 0 \quad (4.4)$$

with

$$U = 0$$

and

$$\int_{-1}^{+1} \bar{z} G * \left\{ \frac{(1-2\nu)}{2L^2} h \cdot \bar{z} \cdot \frac{\partial^2 U}{\partial \eta^2} \right\} d\bar{z} = -3\alpha_0 \int_{-1}^{+1} \bar{z} G * \theta d\bar{z} \quad (4.5)$$

at $\eta = 0$ and $\eta = 1$.

Also, the function $v^{(m)}$ is chosen to satisfy the elastic vibration problem

$$\frac{d^4 v^{(m)}}{d\eta^4} = \frac{4\rho AL^4}{bh^3(1+\nu)} \cdot \omega^2 \cdot v^{(m)} \quad (4.6)$$

with

$$v^{(m)} = 0$$

and

$$\frac{\partial^2 v^{(m)}}{\partial \eta^2} = 0 \quad (4.7)$$

at $\eta = 0$ and $\eta = 1$, where ω is the circular frequency of vibration.

The solution to eqn (4.6) is [18]

$$v^{(m)} = C_m \sin m\pi\eta \quad (4.8)$$

where the constant C_m can be taken as unity without loss of generality.

Substituting eqn (4.3) into eqn (4.1) and using eqns (4.4)–(4.7) and the orthogonal property of $v^{(m)}$ the equation for the “reduced dynamic” solution q_m becomes

$$\frac{d^2 q_m}{dt^2} + \frac{C_p}{\rho A} \frac{dq_m}{dt} + m^4 \pi^4 \frac{bh^3(1+\nu)}{4\rho AL^4} \int_{-1}^{+1} \bar{z}^2 G * q_m(t) d\bar{z} = -2 \int_{-1}^{+1} v^{(m)} \frac{\partial^2 U}{\partial t^2} d\eta \quad (4.9)$$

with the initial conditions

$$q_m(0) = \frac{\int_V \{w(x, 0) - U(x, 0)\} v^{(m)}(x) dV}{\int_V v^{(m)}(x) \cdot v^{(m)}(x) \cdot dV}$$

and

$$\dot{q}_m(0) = \frac{\int_V \{\dot{w}(x, 0) - \dot{U}(x, 0)\} v^{(m)}(x) dV}{\int_V v^{(m)}(x) \cdot v^{(m)}(x) \cdot dV} \quad (4.10)$$

where $w(x, 0)$ and $\dot{w}(x, 0)$ are the known initial conditions of eqn (4.1).

Hence the solution to eqn (4.1) reduces to solving the eqns (4.4) and (4.9) with the appropriate boundary and initial conditions.

4.1.1 *Solution method for the “static” equation.* Equation (4.4) represents the field equation for the “static” part of the problem. Now, defining

$$\int_{-1}^{+1} \bar{z}^2 G * U d\bar{z} = F(\eta, t) \quad (4.11)$$

then the eqn (4.4) becomes

$$\frac{d^4 F}{d\eta^4} = 0 \quad (4.12)$$

along with the boundary conditions

$$F = 0$$

and

$$\frac{\partial^2 F}{\partial \eta^2} = g(t) \quad (4.13)$$

at $\eta = 0$ and $\eta = 1$, where

$$g(t) = \frac{-6\alpha_0 L^2}{(1-2\nu)h} \int_{-1}^{+1} \bar{z} G * \theta(z, t) d\bar{z}$$

The solution to eqn (4.12) is

$$F(n, t) = \frac{\eta}{2} (\eta - 1) \cdot g(t). \quad (4.14)$$

Therefore the solution for U is obtained by solving the integral equation

$$\int_{-1}^{+1} \bar{z}^2 G * U d\bar{z} = -\eta(\eta - 1) \frac{3\alpha_0 L^2}{(1-2\nu)h} \int_{-1}^{+1} \bar{z} G * \theta d\bar{z}. \quad (4.15)$$

The numerical solution to the eqn (4.15) and the algorithm for the finite difference method used in the solution is given in Section 6.

4.1.2 *Solution method for the "reduced dynamic" equation.* Equation (4.9) represents the "reduced dynamic" equation of motion. Substituting eqn (4.8) into eqns (4.9) and (4.10) the "reduced dynamic" equation and the initial conditions become

$$\frac{d^2 q_k}{dt^2} + \frac{C_b}{\rho A} \frac{dq_k}{dt} + \omega_k^2 \int_{-1}^{+1} \bar{z}^2 G * q_k d\bar{z} = -2 \int_0^1 \sin k\pi\eta \cdot \frac{\partial^2 U}{\partial t^2} d\eta \quad (4.16)$$

with

$$q_k(0) = 2 \int_0^1 \sin k\pi\eta \{w(\eta, 0) - U(\eta, 0)\} d\eta$$

and

$$\dot{q}_k(0) = 2 \int_0^1 \sin k\pi\eta \{\dot{w}(\eta, 0) - \dot{U}(\eta, 0)\} d\eta$$

where

$$\omega_k^2 = k^4 \pi^4 \frac{bh^3(1+\nu)}{4\rho AL^4}. \quad (4.17)$$

Now, if the "static solution" U can be expressed in Dirichlet series

$$U(\eta, t) = \eta(\eta - 1) \left\{ U_0 + \sum_{j=1}^J U_j e^{-\beta_j t} \right\}, \quad (4.18)$$

the eqns (4.16) and (4.17) respectively become

$$\frac{d^2 q_k}{dt^2} + \frac{C_b}{\rho A} \frac{dq_k}{dt} + \omega_k^2 \int_{-1}^{+1} \bar{z}^2 G * q_k d\bar{z} = \frac{4}{k^3 \pi^3} (1 - \cos k\pi) \sum \frac{U_j}{\beta_j^2} e^{-\beta_j t} \quad (4.19)$$

and

$$q_k(0) = 2 \int_0^1 \sin k\pi\eta \{w(\eta, 0) - U(\eta, 0)\} d\eta$$

with

$$\dot{q}_k(0) = \frac{4}{k^3 \pi^3} (\cos k\pi - 1) \sum_{j=1}^J \frac{U_j}{\beta_j} + 2 \int_0^1 \sin k\pi\eta \cdot \dot{w}(\eta, 0) d\eta. \quad (4.20)$$

This is an initial value second order integro-differential equation that has been solved using a fourth order Runge-Kutta method. The algorithm and the recursion formula developed in the analysis are presented in Section 6.

4.2 Solution to the equation of motion of a plate

Since the temperature distribution considered (see Section 3) is a function of z and t only, the equation of motion (2.7) becomes

$$\int_{-1}^{+1} \bar{z}^2 D * \nabla^4 w d\bar{z} + \frac{2}{3} \nabla^2 M_T = -\frac{2}{3} \rho h \frac{\partial^2 w}{\partial t^2} - \frac{2}{3} C_p \frac{\partial w}{\partial t} \quad (4.21)$$

where

$$\bar{z} = 2 \frac{z}{h},$$

and

$$M_T = \int_{-1}^{+1} \left(\frac{1+\nu}{h} \right) D * (3\alpha_0 \theta) \bar{z} \, d\bar{z}.$$

The boundary conditions for simply supported edges become

$$w = 0$$

$$\int_{-1}^{+1} \left(D * \frac{\partial^2 w}{\partial x^2} \right) \cdot \bar{z}^2 \, d\bar{z} = -\frac{2}{3} M_T$$

on $x = 0$ and $x = a$, and

$$w = 0$$

$$\int_{-1}^{+1} \left(D * \frac{\partial^2 w}{\partial y^2} \right) \cdot \bar{z}^2 \, d\bar{z} = -\frac{2}{3} M_T \quad (4.22)$$

on $y = 0$ and $y = b$.

Following the eqn (4.3), the solution to the eqn (4.21) can be written as

$$w(x, y, t) = U(x, y, t) + \sum_m \sum_n v^{(m, n)}(x, y) \cdot q_{mn}^{(t)} \quad (4.23)$$

where U the "static solution" satisfies

$$\int_{-1}^{+1} \bar{z}^2 D * \nabla^4 U \, d\bar{z} + \frac{2}{3} \nabla^2 M_T = 0 \quad (4.24)$$

with the boundary conditions

$$U = 0$$

$$\int_{-1}^{+1} \left\{ D * \frac{\partial^2 U}{\partial y^2} \right\} \bar{z}^2 \, d\bar{z} = -\frac{2}{3} M_T$$

on $x = 0$ and $x = a$, and

$$U = 0$$

$$\int_{-1}^{+1} \left\{ D * \frac{\partial^2 U}{\partial y^2} \right\} \bar{z}^2 \, d\bar{z} = -\frac{2}{3} M_T \quad (4.25)$$

on $y = 0$ and $y = b$. Now, $v^{(m, n)}$ is chosen to satisfy the elastic vibration problem

$$\nabla^4 v^{(m, n)} = \lambda v^{(m, n)} \quad (4.26)$$

where

$$\lambda = \pi^4 \left[\left(\frac{m}{a} \right)^2 + \left(\frac{n}{b} \right)^2 \right]^2.$$

The boundary conditions for the above elastic problem are

$$v^{(m, n)} = 0$$

$$\frac{\partial^2 v^{(m, n)}}{\partial x^2} = 0$$

on $x = 0$ and $x = a$, and

$$v^{(m,n)} = 0$$

$$\frac{\partial^2 v^{(m,n)}}{\partial x^2} = 0$$
(4.27)

on $y = 0$ and $y = b$.

The solution to the eqn (4.26) is [18]

$$v^{(m,n)}(x, y) = A_{mn} \sin \frac{m\pi x}{a} \cdot \sin \frac{n\pi y}{b}$$
(4.28)

where A_{mn} can be chosen to be unity without loss of generality.

Substituting eqn (4.23) into (4.21) and using the eqn (4.24) along with the orthogonal property of $v^{(m,n)}$ the equation for "reduced dynamic" solution q_{mn} can be shown to be

$$\frac{2}{3} \rho h \frac{d^2 q_{mn}}{dt^2} + \frac{2}{3} C_p \frac{dq_{mn}}{dt} + \int_{-1}^{+1} \pi^4 \left[\left(\frac{m}{a}\right)^2 + \left(\frac{n}{b}\right)^2 \right] \bar{z}^2 \cdot (D * q_{mn}) d\bar{z}$$

$$= \frac{\int_0^a \int_0^b -\frac{2}{3} \rho h \frac{\partial^2 U}{\partial t^2} \cdot v^{(m,n)}(x, y) dx dy}{\int_0^a \int_0^b v^{(m,n)}(x, y) \cdot v^{(m,n)}(x, y) dx dy}$$
(4.29)

with the initial conditions

$$q_{mn}(0) = \frac{\int_V \{w(x, y, 0) - U(x, y, 0)\} v^{(m,n)}(x, y) dV}{\int_V v^{(m,n)}(x, y) \cdot v^{(m,n)}(x, y) dV}$$

and

$$\dot{q}_{mn}(0) = \frac{\int_V \{\dot{w}(x, y, 0) - \dot{U}(x, y, 0)\} v^{(m,n)}(x, y) dV}{\int_V v^{(m,n)}(x, y) \cdot v^{(m,n)}(x, y) dV}$$
(4.30)

where $w(x, y, 0)$ and $\dot{w}(x, y, 0)$ are the known initial conditions of eqn (4.21).

4.2.1 *Solution method for the "static" equation.* Equation (4.24) represents the field equation for the "static" part of the solution. Now letting

$$\int_{-1}^{+1} \bar{z}^2 D * \nabla^2 U d\bar{z} + \frac{2}{3} M_T = f(x, y)$$
(4.31)

eqn (4.24) can be written as

$$\nabla^2 f = 0$$
(4.32)

and a part of the boundary condition (4.25) yields

$$f = 0$$
(4.33)

on all edges. Hence $f = 0$ everywhere in the domain.

Therefore the field equation becomes

$$\int_{-1}^{+1} D * \left\{ \bar{z}^2 \nabla^2 U + \bar{z} \frac{2(1+\nu)}{h} \alpha_0 \theta \right\} d\bar{z} = 0 \quad (4.34)$$

along with the remaining boundary condition

$$U = 0 \quad (4.35)$$

on the boundaries. Now, defining

$$\bar{U} = \int_{-1}^{+1} D * \bar{z}^2 U d\bar{z},$$

then eqn (4.34) becomes

$$\nabla^2 \bar{U} = g(t) \quad (4.36)$$

where

$$g(t) = \frac{-2(1+\nu)}{h} \alpha_0 \int_{-1}^{+1} \bar{z} D * \theta d\bar{z}$$

along with

$$\bar{U} = 0. \quad (4.37)$$

The solution to eqn (4.36) can be expressed as

$$\bar{U} = \sum_k \sum_l \bar{U}_{kl} \sin \frac{k\pi x}{a} \sin \frac{l\pi y}{b} \quad (4.38)$$

where \bar{U}_{kl} are unknown coefficients to be determined. Now $g(t)$ can be written in a double Fourier series as

$$g(t) = \sum_k \sum_l \frac{4g(t)}{\pi^2 kl} (1 - \cos k\pi)(1 - \cos l\pi) \sin \frac{k\pi x}{a} \sin \frac{l\pi y}{b}. \quad (4.39)$$

Substituting eqns (4.38) and (4.39) into eqn (4.36) the coefficients \bar{U}_{kl} are obtained as

$$\bar{U}_{kl} = -\frac{4}{\pi^2 kl} \frac{g(t)}{\left(\frac{k^2}{a^2} + \frac{l^2}{b^2}\right)} (1 - \cos k\pi)(1 - \cos l\pi).$$

Hence the "static solution" is obtained by solving the equation

$$\int_{-1}^{+1} \bar{z}^2 D * U d\bar{z} = \frac{16}{\pi^2} \frac{2(1+\nu)\alpha_0}{h} \int_{-1}^{+1} \bar{z} D * \theta d\bar{z} \sum_k \sum_l \frac{\sin \frac{k\pi x}{l} \sin \frac{l\pi y}{b}}{kl \left(\frac{k^2}{a^2} + \frac{l^2}{b^2}\right)} \quad (4.40)$$

where $k = 1, 3, 5, \dots$ and $l = 1, 3, 5, \dots$

4.2.2 Solution method for the "reduced dynamic" equation. Equations (4.29) and (4.30) represent the "reduced dynamic" equation of motion for a viscoelastic plate. Expressing the

“static” solution U in a Dirichlet series

$$U = \sum_k \sum_l \frac{\sin \frac{k\pi x}{a} \sin \frac{l\pi y}{b}}{kl \left(\frac{k^2}{a^2} + \frac{l^2}{b^2} \right)} \left[U_0 + \sum_{j=1}^j U_j e^{-\beta_j} \right] \quad (4.41)$$

and substituting in eqns (4.29) and (4.30) along with equation (4.28), the “reduced dynamic” equation and the initial conditions respectively become

$$\frac{d^2 q_{mn}}{dt^2} + \frac{C_p}{\rho h} \frac{dq_{mn}}{dt} + \lambda \int_{-1}^{+1} \bar{z}^2 (G * q_{mn}) d\bar{z} = - \frac{1}{mn \left(\frac{m^2}{a^2} + \frac{n^2}{b^2} \right)} \sum_{j=1}^j \frac{U_j}{\beta_j} e^{-\beta_j} \quad (4.42)$$

where $m, n = 1, 2, \dots$ and

$$\lambda = \left[\frac{m^2}{a^2} + \frac{n^2}{b^2} \right] \frac{h^2 \pi^4}{4\rho(1-\nu)}$$

and

$$q_{mn}(0) = \frac{4}{ab} \int_0^a \int_0^b [w(x, y, 0) - U(x, y, 0)] \sin \frac{m\pi x}{a} \sin \frac{n\pi y}{b} dx dy$$

with

$$\dot{q}_{mn}(0) = \frac{1}{mn \left[\frac{m^2}{a^2} + \frac{n^2}{b^2} \right]} \sum_{j=1}^j \frac{U_j}{\beta_j} + \frac{4}{ab} \int_0^a \int_0^b \dot{w}(z, y, 0) \sin \frac{m\pi x}{a} \sin \frac{n\pi y}{b} dx dy. \quad (4.43)$$

Comparing eqns (4.40) and (4.41) with eqns (4.15) and (4.19) respectively it can be seen that the thermo-viscoelastic beam and plate equations have been expressed in a similar form.

5. EXPERIMENTAL MEASUREMENT OF RELAXATION AND LOG-DECREMENT DATA

5.1 Measurement of relaxation data

5.1.1 *Description of apparatus.* A schematic diagram of the apparatus used for obtaining the torsional relaxation data is shown in Fig. 3. The apparatus consists of a top grip assembly with a balance weight, the specimen and lower grip assembly in an air bearing. The specimen is covered with a tubular, split-wound, power positioning furnace with individual controls for each of the three heating zones. The furnace control has a capacity to maintain a set temperature to within $\pm 0.5^\circ\text{F}$. The bottom shaft of the lower grip assembly is attached to a torque arm through a load transducer. The load transducer consists of a two beam assembly with two strain gages mounted on each one of them. The strain gages are powered using a d.c. power supply and the output amplified by an amplifier before being recorded on a x-y-y recorder. A resistance pot attached in between the lower grip shaft and the torque arm measures the relative change in the applied twist caused by a change in the deflection of the beam due to the relaxation of the material.

5.1.2 *Experimental procedure.* Epoxy† rods of 1.5 in. long and 0.2 in. in dia. were held in the grips. A metallic sleeve was used to completely envelope the specimen to avoid any changes in temperature due to radiation. The specimen was soaked at the required temperature for about an hour after thermal stability was achieved. The temperature measurements were made using thermocouples located as shown in Fig. 3. The torsional loading was developed by rotating the

†The epoxy resin investigated is representative of current high performance composite epoxy matrix resin systems. It contains a multifunctional epoxy (tetraglycidylmethylene dianiline) an aromatic diamine curing agent (diaminodiphenyl-sulfone) and an organometallic catalyst (boron trifluoride complex) and is referred to as 12KV10 in this paper.

torque arm manually and locking the same at a previously determined position. The resistance potentiometer was powered using a 6 V power supply and the strain gages using a HP-311 transducer amplifier indicator. The data was then recorded on a HP-17005A chart recorder. Figure 4 shows the measured data for Hercules 12KV10 epoxy resin. A Dirichlet Series [3] of the type $G(t) = G(0) + \sum_i G_i e^{-t/\tau_i}$ where G_i and τ_i are the spring moduli and relaxation times has been fit for the above measured data and the experimental data obtained by Woo [20] *et al.*, and their results are presented in Tables 1 and 2 respectively.

5.2 Measurement of material damping

Figure 5 shows a schematic view of the experimental setup used for measuring the damping of the epoxy material. Epoxy beams of dimension $5'' \times 5/8'' \times 1/8''$ were clamped at their ends. The beam was forced sinusoidally at a known frequency at the center using an electromagnetic shaker. The output from the force cell and the displacement pickup was then fed to an oscilloscope to obtain a Lissajous pattern. The phase lag determined using the Lissajous pattern was then used to calculate the equivalent log-decrement using the relation

$$\delta = \tan \phi \tag{5.1}$$

where ϕ is the phase angle between the forcing and the displacement functions. The experiment was repeated at various temperatures and frequencies. The magnitude of the stress level was maintained a constant for each temperature level in the specimen.

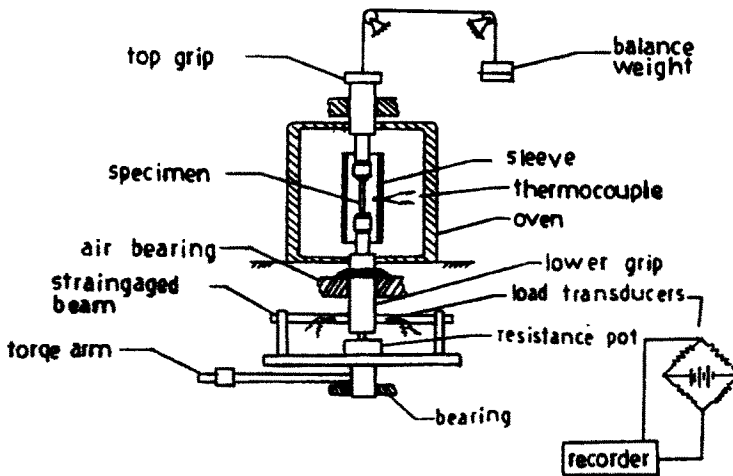


Fig. 3. Apparatus for torsional relaxation measurement.

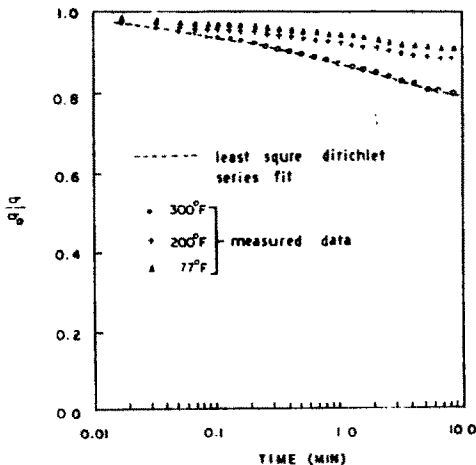


Fig. 4. Torsional relaxation data for epoxy resin (Hercules 12KV10) at different temperatures.

The equivalent log-decrement measured by using the above setup was checked, for a few frequencies, against the values obtained by using the free vibration of a cantilever beam[19]. The results are shown in Table 3.

6. NUMERICAL FORMULATION FOR "STATIC" AND "REDUCED DYNAMIC" EQUATIONS

The integral equations (4.15) and (4.40) are solved in this section using a finite difference discretization in time and space. The "reduced dynamic" equation represented by the two linear second order integro-differential equations (4.19) and (4.42), are solved using a fourth order Runge-Kutta method. The integral operators are expressed in terms of computationally efficient algorithms and the recursion formulae derived where necessary. The computer programs have been written to maintain the accuracy within a given tolerance by comparing the results of the procedure with single and double increment.

Table 1. Least square dirichlet series for epoxy resin (Hercules 12 KV 10)

Temperature °F	Weighting constants		i	τ_i	$G_i/G(0)$
	w_1	w_2			
350°F	0.0	0.0	0	∞	0.7746
			1	5	0.0659
			2	25	0.0281
			3	125	0.0799
			4	500	0.0418
200°F	0.01	0.0	5	750	0.0108
			0	∞	0.8677
			1	5	0.0366
			2	25	0.0111
			3	125	0.0297
77°F	0.01	0.0	4	300	0.0244
			5	600	0.0192
			0	∞	0.8902
			1	5	0.0286
			2	25	0.0077
			3	125	0.0300
			4	300	0.0211
			5	600	0.0132

Table 2. Least square dirichlet series for float glass

i	τ_i	$G_i/G(0)$
0	∞	0.0274
1	1.0	0.1020
2	5.0	0.0231
3	25.0	0.1710
4	125.0	0.3210
5	625.0	0.3740

Base temperature $T_B = 1000^\circ\text{F}$;
 weighting constants: $w_1 = w_2 =$
 0.0; shift function $\phi = 10^{\psi} =$
 $10^{[0.02416(T - T_B)]}$.

Table 3. Comparison of log decrement obtained using cantilever beams for epoxy resin (KV 10) (based on equivalent single degree of freedom analysis)

Temperature (°F)	Frequency (Hz)	Clamped beam (forced vibration)	Cantilever (free vibration)
77	28.80	0.130	0.153
200	27.15	0.140	0.146
350	21.94	0.135	0.121

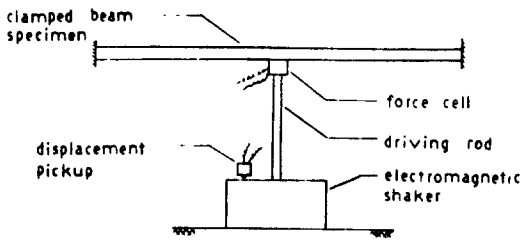


Fig. 5. Experimental apparatus for measuring the damping in epoxy beams.

6.1 *Reduced time evaluation*

The reduced time is given by the eqn (2.3) in the form

$$\xi(z_n, t) = \int_0^t \phi[T(z_n, t')] dt' \tag{6.1}$$

where $\phi(T)$ is the shift factor, a characteristic of the material. To avoid any roundoff errors when successive values are subtracted, changes in reduced time are calculated using

$$\Delta\xi(z_n, t_p) = \int_{t_{p-1}}^{t_p} \phi[T(x_k, t')] dt'. \tag{6.2}$$

The reduced time parameter $\xi(z_n, t_p)$ at any time t_p is then given by

$$\xi(z_n, t_p) = \xi(z_n, t_{p-1}) + \Delta\xi(z_n, t_p) \tag{6.3}$$

with the initial value $\xi(z_n, 0) = 0$. For brevity, the notation $\xi_{n,p}$ will be used to represent the reduced time parameter $\xi(z_n, t_p)$.

The trapezoidal rule approximation for integrating equation (6.2) has been successfully used by Frutiger and Woo[4]. Since the time increment considered here is small, following a similar approach eqn (6.3) can be expressed as

$$\xi_{n,p} = \xi_{n,p-1} + \frac{\Delta t_p}{2} \{\phi_{n,p} + \phi_{n,p-1}\}. \tag{6.4}$$

6.2 *Algorithm for "static" solution*

Equations (4.15) and (4.40) are equivalent except for a function involving the space co-ordinates. This function will be a constant when evaluated at a particular point in the beam/plate. Hence only the development of an algorithm for a beam will be presented here.

Removing the singularity at $t = 0$, eqn (4.15) can be written as

$$\begin{aligned} & \int_{-1}^{+1} \bar{z}^2 \cdot G(\xi) \cdot U(0) d\bar{z} + \int_{-1}^{+1} \bar{z}^2 \int_{0^+}^t G(\xi - \xi') \frac{\partial U}{\partial t'} dt' d\bar{z} \\ & = -\eta(\eta - 1) \frac{3\alpha_0 L^2}{(1 - 2\nu)h} \int_{-1}^{+1} \bar{z} G(\xi) \cdot \theta(0) \cdot dt' \cdot d\bar{z} \\ & \quad - \eta(\eta - 1) \frac{3\alpha_0 L^2}{(1 - 2\nu)h} \int_{-1}^{+1} \bar{z} \int_{0^+}^t G(\xi - \xi') \frac{\partial \theta}{\partial t'} dt' d\bar{z}. \end{aligned} \tag{6.5}$$

But, the temperature distribution (see Section 3) is

$$\theta = T - T_1 = \left[\frac{1}{2}(1 - \bar{z}) - \frac{2}{\pi} \sum_m \frac{1}{m} \exp\left(\frac{-m^2 \pi^2 \bar{a} t}{h^2}\right) \sin \frac{m\pi}{2} (\bar{z} + 1) \right]. \tag{6.6}$$

Therefore, substituting eqn (6.6) into eqn (6.5) and expressing the relaxation modulus $G(t)$ in a Dirichlet Series as

$$G(t) = G_0 + \sum_i G_i e^{-t/\tau_i}$$

where G_i and τ_i are the spring moduli and relaxation times, the left side of the eqn (6.5) becomes

$$\begin{aligned} \frac{2}{3} G_0 U(t_p) + \frac{\Delta \bar{z}}{2} \sum_n \sum_{q=1}^p \sum_i \frac{G_i}{2} [U(t_q) - U(t_{q-1})] \{ \bar{z}_n^2 e^{-\xi_{n,p}/\tau_i} (e^{\xi_{n,q}/\tau_i} \\ + e^{\xi_{n,q-1}/\tau_i}) + \bar{z}_n^2 e^{-\xi_{n-1,p}/\tau_i} (e^{\xi_{n-1,q}/\tau_i} + e^{\xi_{n-1,q-1}/\tau_i}) \} \end{aligned} \quad (6.7)$$

where linear variation of the displacement has been assumed over every interval of the time increment.

To separate the history effects from the rest of the expression define

$$DU^i(n, p) = \sum_{q=1}^p \Delta U_q \{ e^{-\xi_{n,p}/\tau_i} (e^{\xi_{n,q}/\tau_i} + e^{\xi_{n,q-1}/\tau_i}) \} \quad (6.8)$$

where $\Delta U_q = U(t_{q-1})$. The advantage of the above expression is that it can be used to develop a recursion formula which eliminates the history storage. Evaluating the eqn (6.8) at t_{p-1} and comparing the resulting equation with that for t_p , the expression (6.8) can be written as

$$DU^i(n, p) = \Delta U_p (1 + e^{-(\xi_{n,p} - \xi_{n,p-1})/\tau_i}) + e^{-(\xi_{n,p} - \xi_{n,p-1})/\tau_i} DU^i(n, p-1) \quad (6.9)$$

with the initial value $DU^i(n, 0) = 0$.

Hence the expression (6.7) becomes

$$\frac{2}{3} G_0 U(t_p) + \frac{\Delta \bar{z}}{2} \sum_n \sum_i \frac{G_i}{2} [\bar{z}_n^2 DU^i(n, p) + \bar{z}_{n-1}^2 DU^i(n-1, p)]. \quad (6.10)$$

Following the above steps the right side of the eqn (6.5) can be expressed as

$$\begin{aligned} \eta(\eta-1) \frac{3\alpha_0 L^2}{(1-2\nu)h} 4(T_2 - T_1) \frac{G_0}{\pi^2} \sum_m \frac{1}{m^2} (1 - e^{(-m^2 \pi^2 \bar{a}/h^2)t_p}) (1 + \cos m\pi) \\ - \eta(\eta-1) \frac{3\alpha_0 L^2}{(1-2\nu)h} 2(T_2 - T_1) \frac{\pi \bar{a}}{h^2} \sum_i \sum_m \sum_{q=1}^p \sum_n G_i \frac{\Delta \bar{z}}{2} m \frac{\Delta t_q}{2} \left[\bar{z}_n \right. \\ \left. \sin \frac{m\pi}{2} (1 + \bar{z}_n) \cdot e^{-\xi_{n,p}/\tau_i} \left\{ e^{\xi_{n,q}/\tau_i} \cdot e^{(-m^2 \pi^2 \bar{a}/h^2)t_q} + e^{\xi_{n,q-1}/\tau_i} \cdot e^{(-m^2 \pi^2 \bar{a}/h^2)t_{q-1}} \right\} \right. \\ \left. + \bar{z}_{n-1} \sin \frac{m\pi}{2} (1 + \bar{z}_{n-1}) e^{-\xi_{n-1,p}/\tau_i} \left\{ e^{\xi_{n-1,q}/\tau_i} \cdot e^{(-m^2 \pi^2 \bar{a}/h^2)t_q} + e^{\xi_{n-1,q-1}/\tau_i} \cdot e^{(-m^2 \pi^2 \bar{a}/h^2)t_{q-1}} \right\} \right]. \end{aligned} \quad (6.11)$$

Now, defining

$$E^i(m, n, p) = \sum_{q=1}^p \frac{\Delta t_q}{2} e^{-\xi_{n,p}/\tau_i} \{ e^{\xi_{n,q}/\tau_i} \cdot e^{(-m^2 \pi^2 \bar{a}/h^2)t_q} + e^{\xi_{n,q-1}/\tau_i} \cdot e^{(-m^2 \pi^2 \bar{a}/h^2)t_{q-1}} \} \quad (6.12)$$

where $\Delta t_q = t_q - t_{q-1}$, the recursion formula for time integration can be written as

$$\begin{aligned} E^i(m, n, p) = \frac{\Delta t_p}{2} e^{-\xi_{n,p}/\tau_i} \{ e^{\xi_{n,p}/\tau_i} e^{(-m^2 \pi^2 \bar{a}/h^2)t_p} + e^{\xi_{n,p-1}/\tau_i} e^{(-m^2 \pi^2 \bar{a}/h^2)t_{p-1}} \} \\ + e^{-(\xi_{n,p}/\tau_i + \xi_{n,p-1})/\tau_i} E^i(m, n, p-1), \text{ with } E^i(m, n, 0) = 0. \end{aligned} \quad (6.13)$$

Hence the expression (6.11) becomes

$$\begin{aligned} & \eta(\eta - 1) \frac{3\alpha_0 L^2}{(1 - 2\nu)h} 4(T_2 - T_1) \frac{G_0}{\pi^2} \sum_m \frac{1}{m^2} (1 - e^{(-m^2 \pi^2 \bar{a} / h^2) t_p}) (1 + \cos m\pi) - \\ & \eta(\eta - 1) \frac{3\alpha_0 L^2}{(1 - 2\nu)h} 2(T_2 - T_1) \frac{\pi \bar{a}}{h^2} \frac{\Delta z}{2} \sum_m \sum_n \sum_l G_l m \left[\bar{z}_n \sin \frac{m\pi}{n} (\bar{z}_n + 1) \right. \\ & \left. E^i(m, n, p) + \bar{z}_{n-1} \sin \frac{m\pi}{2} (\bar{z}_{n-1} + 1) \cdot E^i(m, n - 1, p) \right] \end{aligned} \tag{6.14}$$

Now, substituting expressions (6.10) and (6.14) into eqn (6.5) the complete algorithm for "static" solution becomes

$$\begin{aligned} & \frac{2}{3} G_0 U(t_p) + [U(t_p) - U(t_{p-1})] + \frac{\Delta \bar{z}}{2} \sum_n \sum_l \frac{G_l}{2} \{ \bar{z}_n^2 (1 + e^{(-\epsilon_{n,p} + \epsilon_{n,p-1}) / \tau_i}) \\ & + \bar{z}_{n-1}^2 (1 + e^{(-\epsilon_{n-1,p} + \epsilon_{n-1,p-1}) / \tau_i}) \} = - \frac{\Delta z}{2} \sum_m \sum_l \frac{G_l}{2} [\bar{z}_n^2 e^{(-\epsilon_{n,p} + \epsilon_{n,p-1}) / \tau_i} \\ & DU^i(n, p - 1) + \bar{z}_{n-1}^2 e^{(-\epsilon_{n-1,p} + \epsilon_{n-1,p-1}) / \tau_i} DU^i(n - 1, p - 1)] + K1 4(T_2 - T_1) \\ & \frac{G_0}{\pi^2} \sum_m \frac{1}{m^2} (e^{(-m^2 \pi^2 \bar{a} / h^2)} - 1) (1 + \cos m\pi) + K1 2(T_2 - T_1) \frac{\pi \bar{a}}{h^2} \frac{\Delta z}{2} \sum_n \sum_l \sum_m G_l m \\ & \left[\bar{z}_n \sin \frac{m\pi}{2} (\bar{z}_n + 1) E^i(m, n, p) + \bar{z}_{n-1} \sin \frac{m\pi}{2} (\bar{z}_{n-1} + 1) E^i(m, n - 1, p) \right] \end{aligned} \tag{6.15}$$

where

$$K1 = - \eta(\eta - 1) \frac{3\alpha_0 L^2}{(1 - 2\nu)h}$$

6.3 Algorithm for "reduced dynamic" solution

Since eqns (4.19) and (4.42) are equivalent except for the coefficients and a function involving the space co-ordinates, the development of algorithm for eqn (4.19) will be presented here.

Considering the initial conditions

$$w(\eta, 0) = \sin \pi \eta$$

and

$$\dot{w}(\eta, 0) = 0 \tag{6.16}$$

to study the free vibration of a beam, eqn (4.20) can be written as

$$q_k(0) = 1$$

with

$$q_k(0) = \frac{4}{k^3 \pi^3} (\cos k\pi - 1) \sum_{j=1}^J \frac{U_j}{\beta_j} \tag{6.17}$$

Now, defining

$$q_k^{(2)} = \dot{q}_k^{(1)} = \frac{dq_k^{(1)}}{dt} \tag{6.18}$$

then eqn (4.19) can be expressed by two first order equations as

$$\frac{dq^{(1)}}{dt} = q^{(2)}$$

with

$$\frac{dq^{(2)}}{dt} = -\frac{4}{k^3 \pi^3} (\cos k\pi - 1) \sum_{j=1}^J \frac{U_j}{\beta_j^2} e^{-j\beta_j} - \omega^2 \int_{-1}^{+1} \bar{z}^2 G * q^{(1)} d\bar{z} - \frac{C_b}{\rho A} \cdot q^{(2)} \tag{6.19}$$

where the subscript k has been omitted for simplicity.

Following the steps given in Section 5.2, the set of eqns (6.19) can be expressed as

$$\frac{dq^{(1)}}{dt} = q^{(2)}$$

and

$$\begin{aligned} \frac{dq^{(2)}}{dt} = & -\frac{4}{k^3 \pi^3} (\cos k\pi - 1) \sum_{j=1}^J \frac{U_j}{\beta_j^2} e^{-j\beta_j} - \omega^2 \frac{2}{3} G_0 q^{(1)}(t_p) - \omega^2 q^{(1)}(0) \frac{\Delta \bar{z}}{2} \\ & \sum_n \sum_i G_i \{ \bar{z}_n^2 e^{-\epsilon_{n,p}/\tau_i} + \bar{z}_{n-1}^2 e^{-\epsilon_{n-1,p}/\tau_i} \} - \omega^2 \frac{\Delta \bar{z}}{2} \sum_n \sum_i \frac{G_i}{2} \{ \bar{z}_n^2 DQ_i(n, p) \\ & + \bar{z}_{n-1}^2 DQ_i(n-1, p) \} - \frac{C_b}{\rho A} \cdot q^{(2)}(t_p) \end{aligned} \tag{6.20}$$

where

$$DQ^i(n, p) = \sum_{m=1}^p \Delta q_m^{(1)} \{ e^{-\epsilon_{n,p}/\tau_i} (e^{\epsilon_{n,m}/\tau_i} + e^{\epsilon_{n,m-1}/\tau_i}) \}$$

and

$$\Delta q_m^{(1)} = q^{(1)}(t_m) - q^{(1)}(t_{m-1}).$$

The recursion formula for time integration will be

$$DQ^i(n, p) = \Delta q_p^{(1)} (1 + e^{(-\epsilon_{n,p} + \epsilon_{n,p-1})/\tau_i}) - e^{(-\epsilon_{n,p} + \epsilon_{n,p-1})/\tau_i} DQ^i(n, p-1). \tag{6.21}$$

The initial conditions for the eqn (6.20) are given by equation (6.17). A fourth order Runge-Kutta approximation has been used to solve the above set of equations.

7. DISCUSSION AND CONCLUSIONS

The difficulty one faces in handling the solution to a thermoviscoelastic problem is mainly due to incorporating the constitutive equation, which is in an integral form, into the equation of motion and then satisfying the resulting nonhomogeneous boundary conditions. Also, the effectiveness of any numerical solution to a particular problem depends on the material characterization. Once a viscoelastic problem involves temperature as a function of space co-ordinates, the material property will also become a function of space coordinates in addition to time. This is the main obstacle in obtaining any type of closed form solution.

The use of the Williams-type modal expansion technique for splitting the solution into a static and dynamic part reduces the computational time and cost for any dynamic problem involving a thermo-viscoelastic material. Also, the convergence of the series evolved in such a method has been shown to be much faster[9] than any other separation technique. The one term approximation used in the present analysis has been found to be more than sufficient for

most engineering applications. This is mainly due to the small magnitude of the amplitude of vibration and its faster rate of decay at higher harmonics.

The present analysis has shown that the use of a Dirichlet series for representation of the material relaxation functions commonly used for the solution of thermoviscoelastic stress problems can also be conveniently used for solving thermoviscoelastic vibration problems. The use of such a series eliminates the history storage thereby reducing the computational time and cost. Such a representation was found to be more realistic than curve fitting the data by means of polynomial approximations.

Figure 6 is a cubic spline fit for the decay of the amplitude of vibration at the mid point of a simply supported float glass beam. At lower temperatures the beam tends to remain elastic in nature for a longer period of time. However, at higher temperatures, the material property starts off elastically and falls down very rapidly with time. As can be seen in Fig. 6, all the curves follow elastic beam vibration initially and diverge as the time progresses.

Figure 7 shows the time dependent vibration of the mid point of a simply supported float glass beam for the temperature extremes considered in this analysis. Even though the temperature differential through the thickness is held constant, the change in the initial temperature appears to induce a small change in the natural frequency of vibration.

Figures 8 and 9 respectively show the amplitude decay and the time dependent motion for a typical float glass plate.

In all of the above discussions only the viscoelastic effect on the free vibration response of beams and plates has been considered. It is well known that all materials exhibit damping, called the internal damping, during any cyclic loading of the material. Figures 10-12 compare

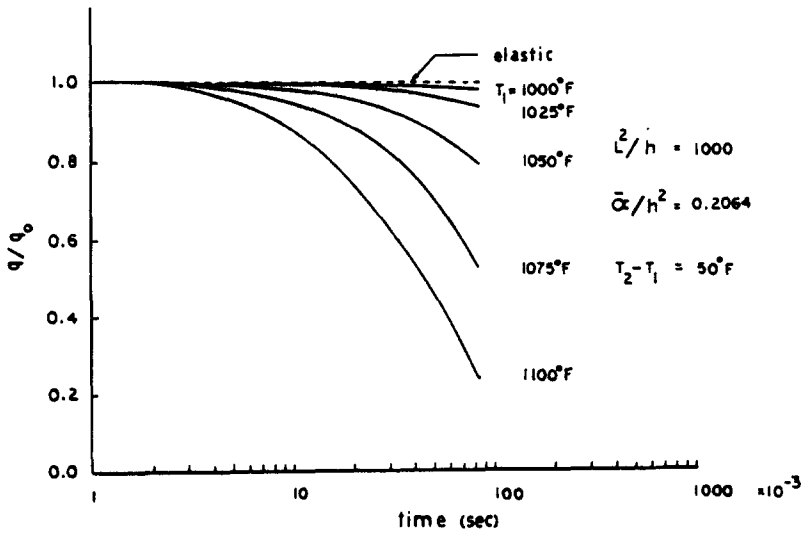


Fig. 6. Mechanical vibration decay of the midpoint of a simply supported float glass beam (envelope of peaks).

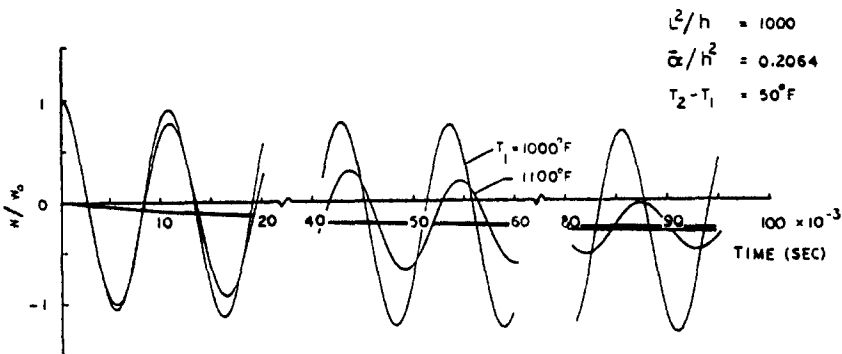


Fig. 7. Time dependent vibrations of the midpoint of a simply supported float glass beam.

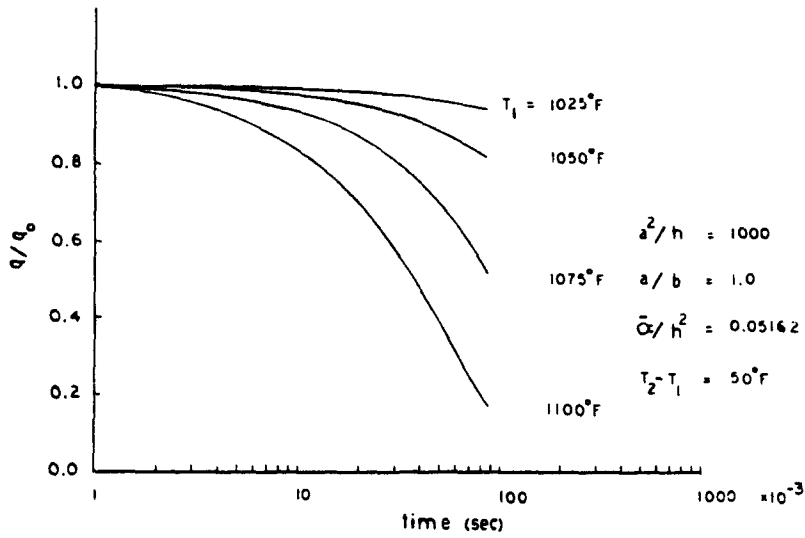


Fig. 8. "Reduced dynamic" vibration of the midpoint of a simply supported float glass plate (envelopes of peaks).

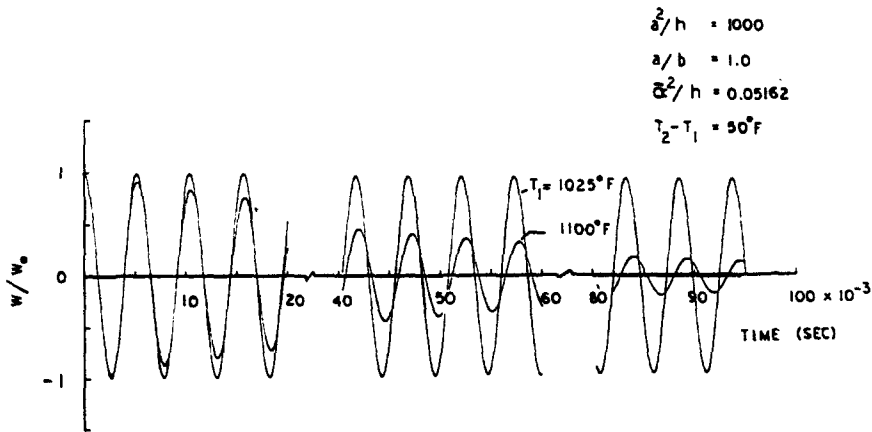


Fig. 9. Time dependent vibration of the midpoint of a simply supported float glass plate.

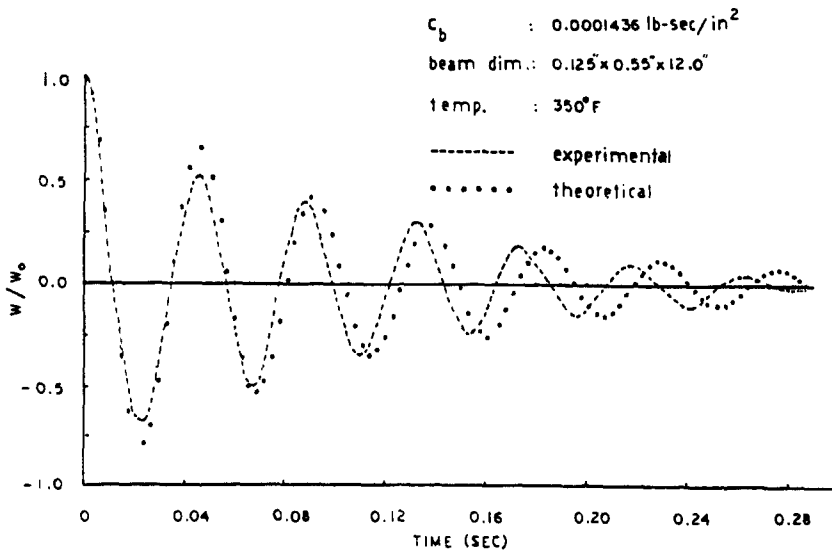


Fig. 10. Comparison of experimental and theoretical free vibrations of the midpoint of a simply supported epoxy resin beam.

the experimentally measured and theoretically obtained free vibration beam midpoint response of epoxy resin simply supported beams at constant temperature. The theoretical results were calculated by taking both material relaxation and internal damping into consideration. Comparison of the results show that the modeling of damping for beams and plates, as derived in Appendix A is a reasonable way of handling the internal damping in viscoelastic materials.

Figures 13 and 14 compare the vibration decay of a simply supported float glass beam. Since damping data [21] for float glass was not available at the temperature considered in the analysis, an upper bound was considered for its value. It can be seen from Fig. 13 that, for float glass, the internal damping does not have much effect on the decay of the amplitude of vibration.

Although it is known that damping is a function of frequency and temperature, the effect of temperature distribution on damping has not been considered, it is expected that the damping remains fairly constant.

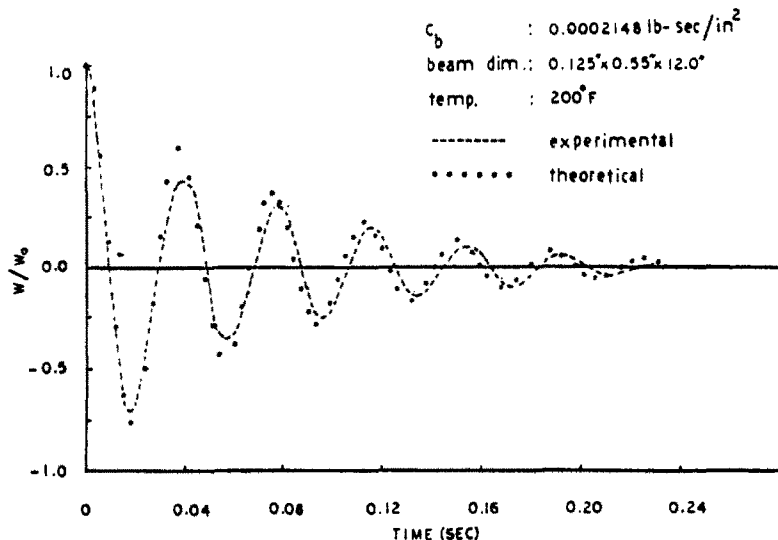


Fig. 11. Comparison of experimental and theoretical free vibration response of a simply supported epoxy resin beam.

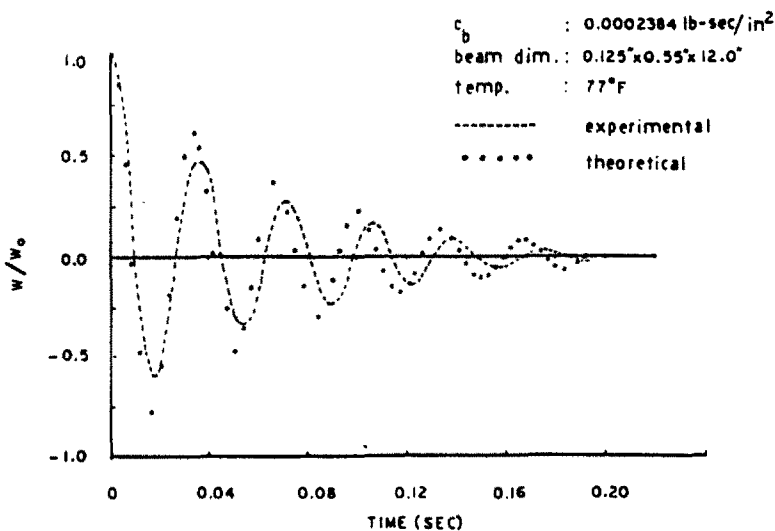


Fig. 12. Comparison of experimental and theoretical free vibration response of a simply supported epoxy resin beam.

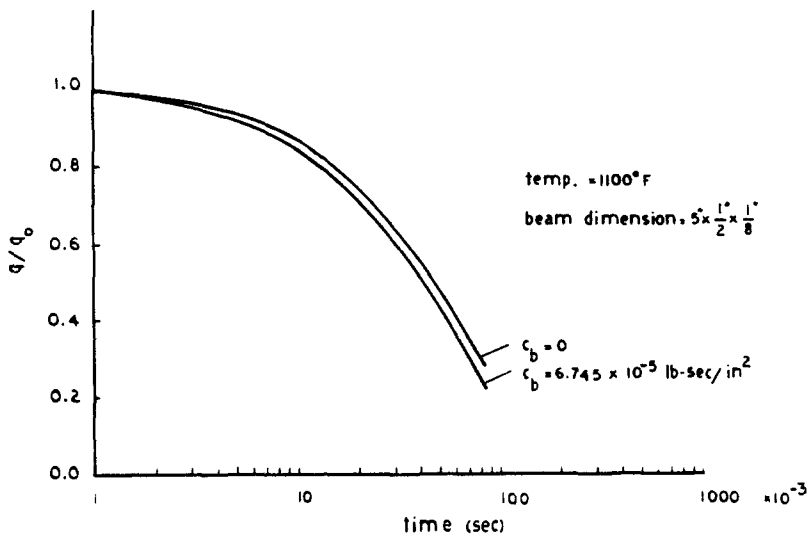


Fig. 13. Dynamic response of a simply supported float glass beam (envelope of peaks).

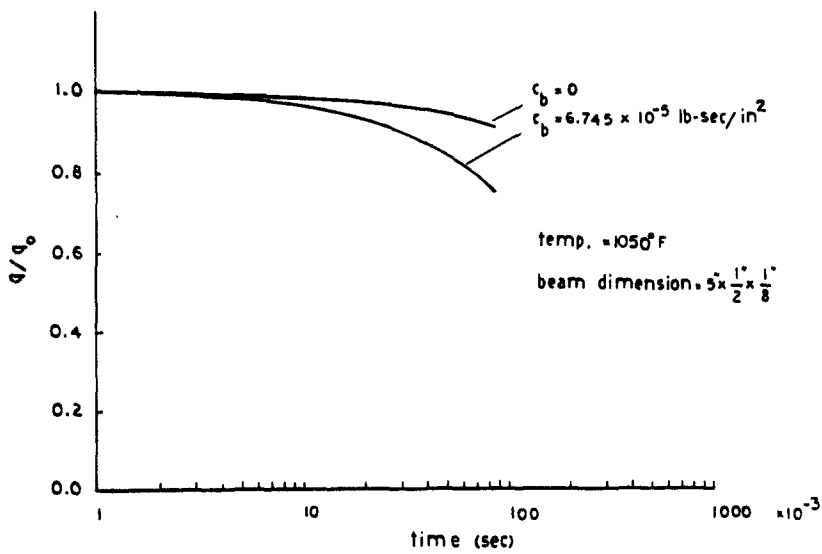


Fig. 14. Dynamic response of a simply supported float glass beam (envelope of peaks).

Table 4. First natural frequency for float glass beams (Hz)

Material	L^2/h	T_1 (°F)	$T_2 - T_1$ (°F)		
			50	75	100
Elastic	1000	—	92.5800	92.5800	92.5800
V.E.†	($h = 0.005''$)	1000	93.7507	—	93.7501
V.E.		1025	93.7507	—	93.3611
V.E.		1050	93.7507	93.3611	92.9753
V.E.		1075	92.9705	—	91.8369
V.E.		1100	91.6498	—	—
Elastic	750	—	123.4380	123.4380	123.4380
V.E.	($h = 0.05''$)	1000	125.0001	—	—
V.E.		1025	125.0001	—	—
V.E.		1050	124.7403	—	—
V.E.		1075	124.2238	—	—
V.E.		1100	122.6996	—	—

†Viscoelastic.

Table 5. First natural frequency for float glass plates (Hz)

Material	a^2/h	a/b	T_1 (°F)	$T_2 - T_1$ (°F)		
				50	75	100
Elastic	1000	1.00	—	189.807	189.807	189.807
V.R.†	($h = 0.1''$)		1025	191.919	—	191.533
V.E.			1050	191.919	—	191.147
V.E.			1075	191.533	191.147	190.381
V.E.	1100	190.381	—	—	—	—
Elastic	1000	0.50	—	118.630	118.630	118.630
V.E.	($h = 0.1''$)		1025	120.000	—	—
V.E.			1050	120.000	—	—
V.E.			1075	119.565	—	—
V.E.			1100	118.535	—	—

†Viscoelastic.

Tables 4 and 5 tabulate the natural frequency for float glass beams and plates of various sizes and temperatures. The changes seen are very small. The natural frequencies for such viscoelastic materials can therefore be approximately calculated using the elastic material properties at the temperature under consideration.

Acknowledgement—The authors wish to thank Dr. T. C. Woo and Dr. N. H. Wackenhut for their helpful discussions during the present work.

REFERENCES

1. R. M. Christensen, *Theory of Viscoelasticity: An Introduction*. Academic Press, New York (1971).
2. Z. P. Bazant and S. T. Wu, Rate-type creep law of aging concrete based on Maxwell chain. *Materiaux et Construction* 7, 37 (1974).
3. Z. P. Bazant and S. T. Wu, Dirichlet series creep functions for aging concrete, *Proc. ASCE, J. Engng Mech. Div.* 99, EM2 (1973).
4. R. L. Frutiger and T. C. Woo, A thermoviscoelastic analysis for circular plates of thermorheologically simple material. *J. Thermal Stresses* 2, 1 (1978).
5. I. M. Daniel, Experimental methods for dynamic stress analysis in viscoelastic materials. *J. Appl. Mech.* 32, 3 (1965).
6. E. F. M. Winter, Viscoelastic characterization of a high performance epoxy resin. Unpublished Masters Thesis, University of Pittsburgh (1979).
7. K. C. Valanis, Exact and variational solutions to a general viscoelastic-kinetic problem. *Trans. ASME, J. Appl. Mech.* 33, 4 (1966).
8. S. R. Robertson, Solving the problem of forced motion of viscoelastic plates by Valanis method with an application to a circular plate. *J. Sound Vib.* 14, 3 (1971).
9. D. Williams, Displacements of a linear elastic system under a given transient load. *Aeronautical Quart.* 1, 2 (1949).
10. R. W. Leonard, One solution for the transient response of beams. NASA R-21 (1959).
11. H. Reismann, Forced motion of elastic plates. *J. Appl. Mech.* 35, 3 (1968).
12. S. R. Robertson, Forced axisymmetric motion of circular viscoelastic plates. *J. Sound Vib.* 17, 3 (1971).
13. S. R. Robertson and C. R. Thomas, Forced motion of viscoelastic solid. *J. Acoust. Soc. Amer.* 49, 5 (1971).
14. B. J. Lazan, *Damping of Materials and Members in Structural Mechanics*. Pergamon Press, London (1968).
15. J. P. Bandstra, Comparison of equivalent viscous damping and non-linear damping in discrete and continuous vibrating systems. Unpublished Masters Thesis, University of Pittsburgh, 1977.
16. L. W. Morland and E. H. Lee, Stress analysis for linear viscoelastic materials with temperature variation. *Trans. Soc. Rheology* 4, 233 (1960).
17. G. E. Myers, *Analytical Methods in Conduction heat Transfer*. McGraw-Hill, New York (1971).
18. L. Meirovitch, *Analytical Methods in Vibrations*. McMillan, New York (1967).
19. S. P. Timoshenko, D. H. Young and W. Weaver, Jr., *Vibration Problems in Engineering*. Wiley, New York (1974).
20. R. W. Douglas and B. Ellis, *Amorphous Materials*. Relaxation of thermal stress of silicate glasses by T. C. Woo, S. M. Ohlberg, E. R. Michalic and R. A. Stewart. Wiley-Interscience, New York (1972).
21. J. H. Ainsworth and R. E. Moore, The frequency-phase technique for damping measurements applied to several materials at elevated temperature. *Materials Res. Standards* 9, 10 (1969).

APPENDIX A

Equivalent viscous damping for simply supported beams and plates

For any vibrating system the strain generally lags the applied stress by some value. This phenomenon which results in dissipation of energy is termed internal damping. Internal damping for a long time has been modelled using single degree of freedom damping [14] as shown in the Fig. A1. The steady state forced displacement for such a vibrating system can be written as

$$x = x_0 \cos \omega t \quad (A1)$$

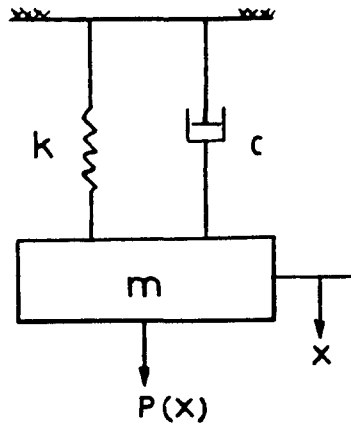


Fig. A1. One dimensional model for viscous damping.

where ω is the excitation frequency. The energy loss per cycle for such a system in steady forced vibration is

$$D = \int_0^{2\pi\omega} c \dot{x}^2 dt \tag{A2}$$

Substituting eqn (A1) into eqn (A2) the energy loss per cycle can be written as

$$D = \pi c x_0^2 \omega \tag{A3}$$

For a simply supported beam the steady state fundamental mode response can be approximated by

$$w(x, t) = w_0 \sin \frac{\pi x}{L} \sin \omega t \tag{A4}$$

where ω is the frequency of excitation. The energy loss per cycle due to internal damping is

$$D = \int_0^L \int_0^{2\pi\omega} C_b \left(\frac{\partial w}{\partial t} \right)^2 dt dx \tag{A5}$$

where C_b is the equivalent viscous damping. Substituting eqn (A4) into (A5), the energy loss will become

$$D = \frac{\pi}{2} w_0^2 \cdot C_b \cdot L \cdot \omega \tag{A6}$$

Equating eqns (A3) and (A6), the coefficient of equivalent viscous damping can be written as

$$C_b = c \frac{x_0^2}{w_0^2} \cdot \frac{2}{L} \tag{A7}$$

Hence, to evaluate the equivalent viscous damping for a simply supported beam, it is necessary to determine the damping coefficient "c" of the corresponding single degree of freedom system at the excitation frequency of the beam.

If the damping coefficient "c" of the single degree of freedom system is determined using log decrement [19] of a tuned cantilever beam, the eqn (A7) reduces to

$$C_b = 23.64 c l L \tag{A8}$$

where L is the length of the simply supported beam.

For a simply supported plate the steady state fundamental mode response can be written as

$$w(x, y, t) = w_0 \sin \frac{\pi x}{a} \cdot \sin \frac{\pi y}{b} \cdot \sin \omega t \tag{A9}$$

Following the steps used for a simply supported beam the coefficient of equivalent viscous damping can be obtained in the form

$$C_p = 4.4995 \cdot c \cdot \frac{ab b^2}{A^2 L^2} \tag{A10}$$

where A and L are respectively the area of cross-section and length of the tuned cantilever beam and a , b and h are the plate dimensions.

In the above analysis, even though the damping is a function of temperature, it has been assumed to be a constant. The error involved due to this assumption is minimal, except near the glass transition temperature.